

RESEARCH

Open Access



# Integrative multi-omics analysis reveals novel idiopathic pulmonary fibrosis endotypes associated with disease progression

Peifeng Ruan<sup>1†</sup>, Jamie L Todd<sup>2,3†</sup>, Hongyu Zhao<sup>1</sup>, Yi Liu<sup>4</sup>, Richard Vinisko<sup>4</sup>, Julia F. Soellner<sup>5</sup>, Ramona Schmid<sup>5</sup>, Robert J. Kaner<sup>6</sup>, Tracy R. Luckhardt<sup>7</sup>, Megan L. Neely<sup>2,3</sup>, Imre Noth<sup>8</sup>, Mary Porteous<sup>9</sup>, Rishi Raj<sup>10</sup>, Zeenat Safdar<sup>11</sup>, Mary E Strek<sup>12</sup>, Christian Hesslinger<sup>5</sup>, Scott M. Palmer<sup>2,3</sup>, Thomas B. Leonard<sup>4</sup> and Margaret L. Salisbury<sup>13\*</sup>

## Abstract

**Background** Idiopathic pulmonary fibrosis (IPF) is characterized by the accumulation of extracellular matrix in the pulmonary interstitium and progressive functional decline. We hypothesized that integration of multi-omics data would identify clinically meaningful molecular endotypes of IPF.

**Methods** The IPF-PRO Registry is a prospective registry of patients with IPF. Proteomic and transcriptomic (including total RNA [toRNA] and microRNA [miRNA]) analyses were performed using blood collected at enrollment. Molecular data were integrated using Similarity Network Fusion, followed by unsupervised spectral clustering to identify molecular subtypes. Cox proportional hazards models tested the relationship between these subtypes and progression-free and transplant-free survival. The molecular subtypes were compared to risk groups based on a previously described 52-gene (toRNA expression) signature. Biological characteristics of the molecular subtypes were evaluated via linear regression differential expression and canonical pathways (Ingenuity Pathway Analysis [IPA]) over-representation analyses.

**Results** Among 232 subjects, two molecular subtypes were identified. Subtype 1 (n = 105, 45.3%) and Subtype 2 (n = 127, 54.7%) had similar distributions of age (70.1 +/- 8.1 vs. 69.3 +/- 7.6 years; p = 0.31) and sex (79.1% vs. 70.1% males, p = 0.16). Subtype 1 had more severe disease based on composite physiologic index (CPI) (55.8 vs. 51.2; p = 0.002). After adjusting for CPI and antifibrotic treatment at enrollment, subtype 1 experienced shorter progression-free survival (HR 1.79, 95% CI 1.28, 2.56; p = 0.0008) and similar transplant-free survival (HR 1.30, 95% CI 0.87, 1.96; p = 0.20) as subtype 2. There was little agreement in the distribution of subjects to the molecular subtypes and the risk groups based on 52-gene signature (kappa = 0.04, 95% CI = -0.08, 0.17), and the 52-gene signature risk groups were associated with differences in transplant-free but not progression-free survival. Based on heatmaps and differential expression analyses, proteins and miRNAs (but not toRNA) contributed to classification of subjects to the molecular

<sup>†</sup>Peifeng Ruan and Jamie L Todd contributed equally.

\*Correspondence:  
Margaret L. Salisbury  
margaret.salisbury@vumc.org

Full list of author information is available at the end of the article



© The Author(s) 2023. **Open Access** This article is licensed under a Creative Commons Attribution 4.0 International License, which permits use, sharing, adaptation, distribution and reproduction in any medium or format, as long as you give appropriate credit to the original author(s) and the source, provide a link to the Creative Commons licence, and indicate if changes were made. The images or other third party material in this article are included in the article's Creative Commons licence, unless indicated otherwise in a credit line to the material. If material is not included in the article's Creative Commons licence and your intended use is not permitted by statutory regulation or exceeds the permitted use, you will need to obtain permission directly from the copyright holder. To view a copy of this licence, visit <http://creativecommons.org/licenses/by/4.0/>. The Creative Commons Public Domain Dedication waiver (<http://creativecommons.org/publicdomain/zero/1.0/>) applies to the data made available in this article, unless otherwise stated in a credit line to the data.

subtypes. The IPA showed enrichment in pulmonary fibrosis-relevant pathways, including mTOR, VEGF, PDGF, and B-cell receptor signaling.

**Conclusions** Integration of transcriptomic and proteomic data from blood enabled identification of clinically meaningful molecular endotypes of IPF. If validated, these endotypes could facilitate identification of individuals likely to experience disease progression and enrichment of clinical trials.

**Trial registration** NCT01915511

**Keywords** Lung fibrosis, Cluster analysis, Biomarkers, Proteomics, RNA, Computational biology

## Background

Idiopathic pulmonary fibrosis (IPF) is characterized by abnormal accumulation of extracellular matrix (ECM) in the pulmonary interstitium. The natural history of IPF is characterized by progressive decline in lung function, often culminating in death from respiratory failure [1]. Significant progress has been made in understanding the pathobiology of IPF, including high-throughput assessments of genetic risk factors, changes in gene expression, and alterations in the abundance of proteins in the lungs or peripheral blood that are associated with the development or progression of IPF [2–11]. These studies reinforce the conceptualization of IPF as a disease initiated by recurrent, low-grade injury to the lung epithelium, with pathologic disruption in cellular aging and innate immune responses to injury as drivers of ECM deposition. Molecular analyses have yielded candidate biomarkers for confirmation of an IPF diagnosis or staging of disease. A 52-gene expression signature [9, 10] and, more recently, a 13-gene signature developed using unsupervised clustering [12], identified persons with IPF at high risk of mortality when measured in peripheral blood. In addition, a signature of 17 proteins measured in peripheral blood identified patients with non-idiopathic pulmonary fibrosis who were at high risk of disease progression [11]. MicroRNAs (miRNAs), small non-coding RNAs that regulate gene expression post-transcription [13], have been mechanistically linked to IPF, but are incompletely studied as biomarkers of disease progression [14–16].

Integrative multi-omics analyses have identified molecular subtypes of several forms of cancer [17–21]. With a few exceptions, high-throughput studies of the molecular landscape of IPF have focused on alterations in a single type of molecule [22–25]. In this study, we measured the abundance of proteins and the expression of total RNA and miRNAs in the peripheral blood of patients with IPF enrolled in a multi-center observational registry. We hypothesized that cross-platform integration and simultaneous assessment of several types of molecules in the gene-to-function pathway using an unsupervised integrative clustering method would identify clinically meaningful molecular endotypes of IPF.

## Methods

This study included 300 patients enrolled in the US-based, multi-center, observational Idiopathic Pulmonary Fibrosis Prospective Outcomes (IPF-PRO) Registry (NCT01915511), whose key inclusion criterion is IPF diagnosed or confirmed at the enrolling center in the past 6 months [26]. Enrollment procedures included collection of a blood sample, demographics and health information. Patients are followed longitudinally with information such as pulmonary function tests collected as part of their routine clinical care. For this analysis, all participants who were enrolled between June 2014 and February 2017, with longitudinal outcomes ascertained through December 2019, and who had blood samples available for molecular analyses described below were selected. A formal power analysis was not conducted.

### Identification of molecular subtypes of IPF

Whole blood and plasma collected at enrollment were stored centrally. The process used to quantify plasma proteins by aptamer-based methods, measure miRNA expression in plasma, sequence total RNA (referred to as toRNA) in whole blood, and to perform bioinformatics analyses, is described in Additional file 1: Section S1. After excluding 52 subjects due to low toRNA quality, 9 due to low miRNA quality, and 7 for low quality of both, data from 232 subjects were analyzed. Additional file 2: Table S1 summarizes the features within each molecule type (toRNA, miRNA, protein) that were available for modeling.

To identify molecular subtypes of IPF, an integrative, two-step method, spectral clustering Similarity Network Fusion (scSNF) was used to cluster subjects based on data from all three molecule types. First, Similarity Network Fusion, a method that integrates similarity networks, was applied to fuse proteomics, miRNA and toRNA expression data for each subject [27]. Second, an unsupervised spectral clustering method [28] was applied to the fused similarity network. This method uses eigenvectors of the graph Laplacian of the similarity network to cluster subjects. To achieve stable clustering results, consensus clustering with 100 iterations and a 0.8 subsampling ratio was applied [29]. Average Silhouette scores [30] were used to determine the number of clusters, with 2 to 10 clusters

assessed, where scores near 1 indicate optimal clustering and a decrease toward 0 indicates increasing overlap in clusters. The scSNF method was compared to the alternative integrative clustering methods iCluster+ [31] and iClusterBayes [32]. Sensitivity analyses assessed clustering membership when the toRNA variance filter (set as the top 10% most variable features for the main analysis) was adjusted to include the top 50% most variable features or to 100%.

### Clinical characterization of molecular subtypes of IPF

Patient characteristics within each molecular subtype were summarized using means and standard deviations for continuous variables and numbers and percentages for categorical variables. Characteristics were compared between the subtypes using the Kruskal-Wallis test for continuous variables and the Chi-square test for categorical variables, with  $p < 0.05$  considered statistically significant. To determine the relationship between the molecular subtypes and clinically meaningful outcomes, the occurrence of two composite outcomes was determined: (1) lung transplant or death; and (2) disease progression, defined as  $\geq 10\%$  absolute decline in forced vital capacity (FVC) % predicted, lung transplant, or death. FVC decline recorded at the first instance of a post-enrollment value  $\geq 10\%$  lower than the enrollment value. These events were selected because they can be objectively assessed and have similar importance in the natural history of IPF [33]. Transplant-free and progression-free survival were considered separately to enable an evaluation of the relationship between molecular markers and these two outcomes. Subjects who withdrew from the study or had not experienced an outcome by December 2019 were censored on the date of their last follow-up visit. Kaplan-Meier plots and Cox proportional hazards regression models (unadjusted, and adjusted for baseline disease severity based on the composite physiologic index [CPI] [34] and antifibrotic treatment status at enrollment) were used to determine the risk of the two composite outcomes.

Next, to place the molecular subtypes identified in this study in the context of existing literature, the previously described 52-gene expression signature was applied to group the subjects as high-risk or low-risk (for death or transplant) [9, 10]. Cohen's kappa assessed agreement in groupings based on the molecular subtypes and the 52-gene signature. The risk of experiencing each composite outcome was assessed for the 52-gene signature high-risk compared to the low-risk group using Kaplan-Meier plots and Cox proportional hazards regression models (unadjusted, and adjusted for CPI and antifibrotic treatment status).

### Biological characterization of molecular subtypes of IPF

The molecular characteristics that distinguished the subtypes identified by scSNF were investigated in several ways. First, Normalized Mutual Information (NMI) measured agreement of distribution of the subjects to the subtypes when clusters were formed using only one data type (i.e., protein, toRNA, or miRNA) compared to using all three data types [35]. Next, heatmaps visualized differences in protein abundance, toRNA, and miRNA expression between the subtypes. Finally, a random forest model [36] with 5-fold cross validation was used to identify molecular features that could classify individuals to a subtype. The classifier process is described in Additional file 3: Section S2 and Figure S1.

To investigate the biology underlying the molecular subtypes, linear regression models identified differentially expressed features within each molecule set (see Additional file 4: Section S3 for details). Then, Ingenuity Pathway Analysis (IPA) (QIAGEN Inc.) [37] identified canonical pathways in which differentially expressed features were significantly over-represented, based on a hypergeometric/right-tailed Fisher's exact test with false discovery rate (FDR)-adjusted  $p$ -value  $< 0.05$  [38]. IPA analyses were conducted separately among significantly up-regulated and down-regulated features. All analyses except those performed with IPA were performed using R version 3.6.1.

## Results

### Unsupervised clustering identified molecular subtypes of IPF with distinct clinical characteristics

The scSNF clustering method suggested two as the optimal number of clusters based on Silhouette scores (Additional file 5: Figure S2). The alternative clustering methods (iCluster+ and iClusterBayes) suggested a larger number of clusters, but these were largely overlapping with the scSNF clusters (Additional file 5: Section S4 and Table S2). In the sensitivity analyses based on different RNA-seq variance filters, scSNF clusters were preserved across variance filtering cutpoints (Additional file 5: Table S3).

Subtype 1 comprised 105 (45.3%) subjects while subtype 2 comprised 127 (54.7%) subjects. Subtype 1 had more severe disease at baseline, with lower diffusion capacity of the lung for carbon monoxide (DLco) % predicted (38.3 vs. 43.1;  $p = 0.01$ ), lower FVC % predicted (67.9 vs. 73.8;  $p = 0.02$ ), and higher CPI (55.8 vs. 51.2;  $p = 0.002$ ). There were no significant differences in age, sex, smoking status, medical history, GAP stage [39], diagnostic category [40], or antifibrotic treatment status at enrollment (Table 1).

During a median follow-up of 27.5 months (interquartile range 15.8–36.7 months), the composite of lung transplant or death occurred in 95 (40.9%) subjects

**Table 1** Patient characteristics at enrollment by molecular subtype

	Subtype 1 (N= 105)	Subtype 2 (N= 127)	p-value <sup>+</sup>
Age	70.08 (8.07)	69.33 (7.62)	0.31
Sex			0.16
M	83 (79.1%)	89 (70.1%)	
F	22 (21.0%)	38 (30.0%)	
Ever smoker			0.59
Y	73 (69.5%)	83 (65.4%)	
N	32 (30.5%)	44 (34.7%)	
History of coronary artery disease (including prior MI)*			1.0
Y	33 (31.4%)	39 (31.0%)	
N	72 (68.6%)	87 (69.1%)	
History of COPD*			1.0
Y	19 (18.1%)	22 (17.5%)	
N	86 (81.9%)	104 (82.5%)	
History of diabetes*			0.18
Y	24 (22.9%)	19 (15.1%)	
N	81 (77.1%)	107 (84.9%)	
Antifibrotic treatment			0.07
Nintedanib	24 (22.9%)	18 (14.17%)	
Pirfenidone	41 (38.1%)	43 (33.86%)	
Neither	40 (39.1%)	66 (52.0%)	
DL <sub>CO</sub> % predicted	38.31 (12.46)	43.09 (14.69)	0.01
FVC % predicted	67.89 (15.18)	73.82 (17.72)	0.02
FEV <sub>1</sub> % predicted	76.09 (16.11)	81.03 (20.00)	0.12
CPI [34]	55.77 (9.93)	51.21 (11.49)	0.01
Diagnostic category [40]			0.41
Definite IPF	77 (73.3%)	95 (74.8%)	
Probable IPF	22 (21.0%)	29 (22.8%)	
Possible IPF	6 (5.7%)	3 (2.4%)	
GAP stage [39]			0.15
1	22 (21.0%)	40 (31.5%)	
2	64 (61.0%)	71 (55.9%)	
3	19 (18.1%)	16 (12.6%)	

Data are mean (SD) or n (%). Abbreviations: MI: Myocardial infarction, DLco: Diffusing capacity of the lungs for carbon monoxide, FVC: Forced vital capacity, FEV<sub>1</sub>: Forced expiratory volume in the first second, CPI: Composite physiologic index.

\*One subject in subtype 1 was missing medical history.

<sup>+</sup>Kruskal-Wallis test compared continuous variables and Chi-square test compared categorical variables.

(18 lung transplants, 77 deaths, and 137 censored non-events). The composite of disease progression occurred in 143 (61.6%) subjects (88 with FVC decline, 8 lung transplants, 47 deaths, and 89 censored non-events). In the unadjusted analysis, subjects in subtype 1 experienced a significantly shorter time to lung transplant or death (median 35 vs. 45 months, log-rank  $p=0.03$ ; HR 1.54, 95% CI 1.03–2.23,  $p=0.03$ ) (Fig. 1A) and a

significantly shorter time to disease progression (median 21 vs. 32 months, log-rank  $p<0.0001$ ; HR 1.96, 95% CI 1.41, 2.78,  $p<0.0001$ ) (Fig. 1B). After adjusting for CPI and antifibrotic treatment status at enrollment, subtype 1 had a significantly shorter time to disease progression (adjusted HR 1.79, 95% CI 1.28, 2.56;  $p=0.0008$ ) but no different time to transplant or death (adjusted HR 1.30, 95% CI 0.87, 1.96;  $p=0.20$ ) (Fig. 1).

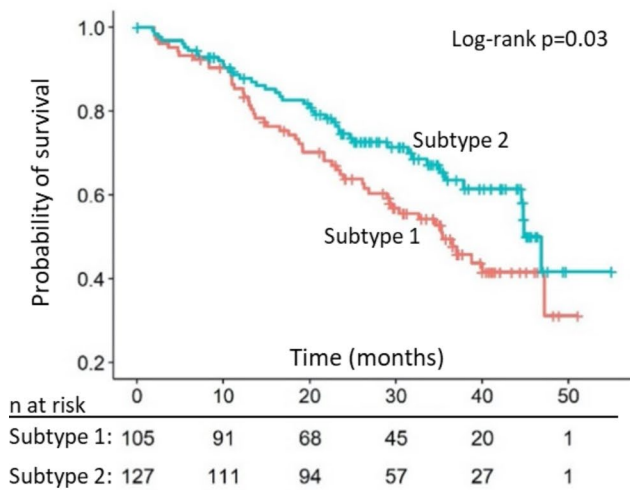
When the 52-gene signature was applied to our analysis cohort, the high-risk group comprised 85 (36.6%) subjects and the low-risk group 147 (63.3%) subjects. The molecular subtypes were distinct from the 52-gene signature risk groups, with no agreement beyond chance ( $k=0.04$ , 95% CI= -0.08, 0.17),  $p=0.49$ ; Additional file 5: Table S4). The 52-gene high-risk group experienced an increased risk of lung transplant or death in unadjusted and adjusted models (Fig. 2A). However, the high-risk group did not experience a significantly increased risk for disease progression in unadjusted or adjusted models (Fig. 2B).

#### Molecular subtypes differed based on proteomics and miRNA features

Based on good agreement (indicating substantial overlap) on the distribution of subjects to a cluster using a single molecule type compared to the scSNF multi-omics data, proteins (NMI=0.41) and miRNAs (NMI=0.62) contributed substantially to the clustering, while toRNAs had little effect (NMI=0.0003) (Additional file 5: Table S5). Heatmaps confirmed this assessment, with clear differences between the subtypes for proteins and miRNAs but not for toRNAs (Fig. 3).

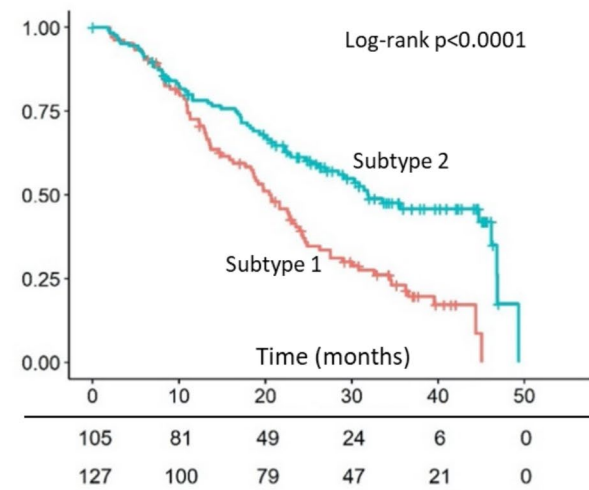
The random forest classifier yielded a 5-iteration mean classifier prediction area AUC of 0.95 (sd=0.03) to predict the molecular subtypes. To further assess the classifier's performance to identify clinically meaningful subtypes of IPE, Cox proportional hazard models estimated the risk to experience each composite endpoint in each iteration's training and validation datasets. Although the classification of subjects to the molecular subtypes based on each iteration's classifier did not achieve  $p<0.05$  in all iterations, the point estimates of HR were in the same direction, suggesting consistent classification of subjects based on clinically meaningful outcomes using the molecular data (Fig. 4). Features selected at least 3 times in all 5 iterations included 34 proteins and 7 miRNAs (see Table 2, including the mean variable importance for each molecule), and features selected in all 5 iterations included 4 proteins (BARK1, IF4G2, NDP kinase B, UFC1) and 1 miRNA (miR-744-5p).

**A. Composite of lung transplant or death**



Cox PH models	HR (95% CI)	p-value
Unadjusted model: Molecular subtype 1 vs 2	1.54 (1.03, 2.33)	0.03
Adjusted model Molecular subtype 1 vs 2	1.30 (0.87, 1.96)	0.20
CPI, per +1 point	1.09 (1.06, 1.11)	<0.0001
Antifibrotic treatment	0.98 (0.65, 1.47)	0.91

**B. Composite of  $\geq 10\%$  decline in FVC % predicted, lung transplant, or death**



Cox PH models	HR (95% CI)	p-value
Unadjusted model: Molecular subtype 1 vs 2	1.96 (1.41, 2.78)	<0.0001
Adjusted Model Molecular subtype 1 vs 2	1.79 (1.28, 2.56)	0.0008
CPI, per +1 point	1.03 (1.02, 1.05)	0.001
Antifibrotic treatment	0.92 (0.66, 1.28)	0.63

**Fig. 1** Risk of outcomes based on the molecular IPF subtype. Kaplan-Meier plots show the time from enrollment to the composite outcome of lung transplant or death (A) and the composite outcome of  $\geq 10\%$  absolute decline in FVC % predicted, lung transplant, or death (B) for subtype 1 compared to subgroup 2. The associated tables show the unadjusted hazard ratio and the hazard ratio adjusted for CPI and antifibrotic treatment use for subtype 1 compared to subtype 2. HR: hazard ratio; PH: proportional hazards; CPI: composite physiologic index

**Coordinated alteration of biological pathways in the molecular subtypes**

Linear regression identified 232 proteins (Additional file 5: Table S6), 291 miRNAs (Additional file 4: Table S7), and no tRNAs that were significantly differentially expressed or abundant between the molecular subtypes. In the IPA analysis of differentially abundant proteins, 209 down-regulated proteins (in subtype 1 compared to subtype 2) corresponded to 69 enriched pathways (Additional file 6: Table S8). Among the 291 differentially expressed miRNAs, 142 were up-regulated, corresponding to 591 experimentally-validated target genes and 345 significantly enriched pathways, and 149 were down-regulated, corresponding to 1,313 target genes and 341 significantly enriched pathways (Additional file 7: Table S9).

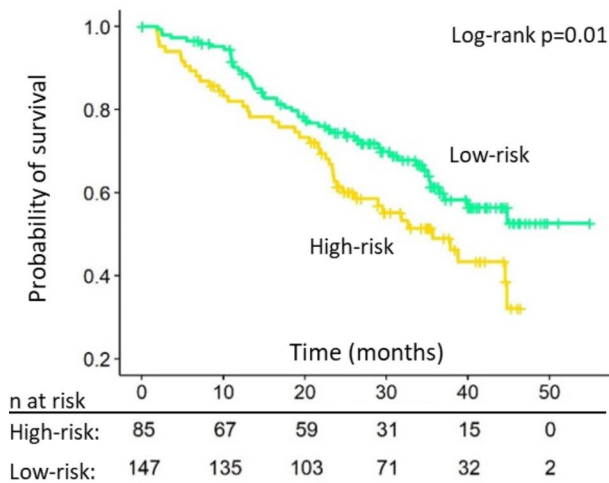
Interestingly, there was substantial overlap in the pathway over-representation analysis for proteins and miRNA target genes (Fig. 5; and see specific pathways highlighted in Table S8 and Table S9). Pathway enrichment shared among down-regulated proteins and up-/down-regulated miRNAs included mTOR, FGF, VEGF, PDGF, ERK/MAPK signaling, NRF2-mediated oxidative

stress response, and PI3K signaling in B lymphocytes. Among enriched pathways that were unique to up-regulated miRNAs, many were related to cellular or metabolic processes, such as endoplasmic reticulum stress pathway, unfolded protein response, NAD salvage pathway II, and glucose and glucose-1-phosphate degradation. Among enriched pathways that were unique to down-regulated miRNAs, many were related to immunity, including altered T and/or B cell signaling, role of RIG1-like receptors in antiviral innate immunity, and crosstalk between dendritic cells and natural killer cells.

**Discussion**

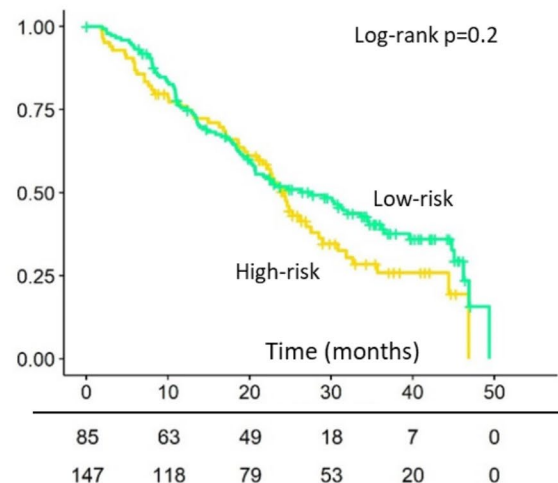
In this analysis of the IPF-PRO Registry, a prospective registry of patients with IPE, we used a two-step method to harmonize multi-omics datasets and conduct unsupervised clustering based on the molecular features. This method identified two novel molecular subtypes of IPF associated with distinct clinical characteristics. Patients in subtype 1 had more severe disease at enrollment and shortened time to disease progression than patients in subtype 2, after adjusting for disease severity and use of

A. Composite of lung transplant or death



Cox PH models	HR (95% CI)	p-value
Unadjusted model: High-risk	1.69 (1.14, 2.56)	0.01
Adjusted model High-risk vs low-risk CPI, per +1 point	1.52 (1.00, 2.27) 1.09 (1.07, 1.12)	0.048 <0.0001
Antifibrotic treatment	1.01 (0.68, 1.52)	0.95

B. Composite of ≥10% decline in FVC % predicted, lung transplant, or death



Cox PH models	HR (95% CI)	p-value
Unadjusted model: High-risk	1.28 (0.91, 1.79)	0.15
Adjusted model High-risk CPI, per +1 point	1.23 (0.88, 1.72) 1.04 (1.02, 1.05)	0.22 <0.0001
Antifibrotic treatment	0.98 (0.70, 1.36)	0.89

**Fig. 2** Risk of outcomes based on the 52-gene signature. Kaplan-Meier plots show the time from enrollment to the composite outcome of lung transplant or death (A) and the composite outcome of ≥ 10% absolute decline in FVC % predicted, lung transplant, or death (B) for the high-risk group and low-risk group. The associated tables show the unadjusted hazard ratio and the hazard ratio adjusted for CPI and antifibrotic treatment use for the high-risk group compared to the low-risk group. HR: hazard ratio; PH: proportional hazards; CPI: composite physiologic index

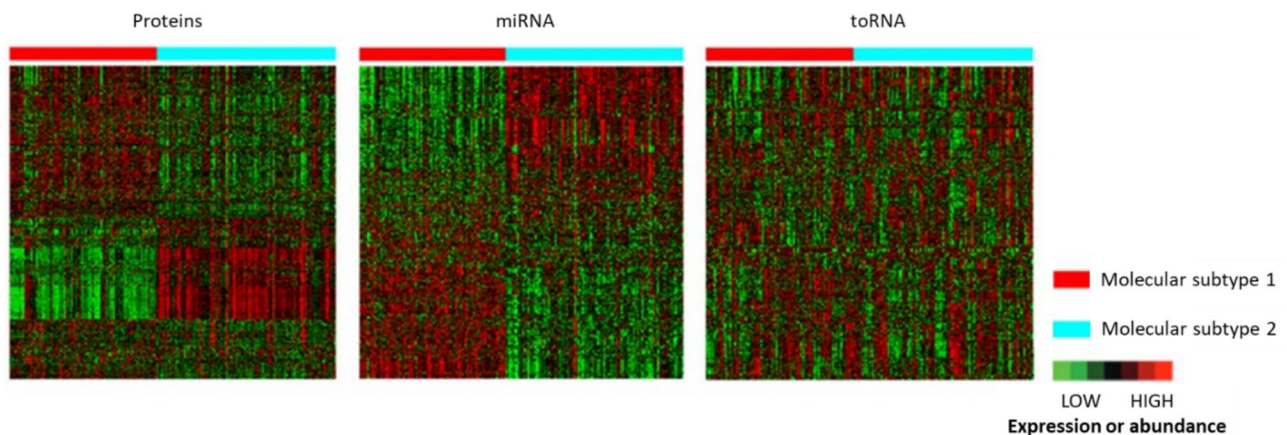


**Fig. 3** Heatmaps comparing protein abundance and miRNA or toRNA expression in the molecular IPF subtypes determined by the spectral clustering Similarity Network Fusion (scSNF) integrated two-step method

antifibrotic treatment at baseline. The distribution of subjects into the molecular subtypes was driven by miRNA expression and protein abundance, while toRNA expression did not differ between the subtypes. Consistent with this observation, these molecular subtypes of IPF were distinct from risk groups identified using a previously

described 52-gene (RNA) signature [9, 10]. A signature of 34 circulating proteins and 7 circulating miRNAs may be useful to classify patients as subtype 1 or 2. These data will be important to permit validation of the existence and clinical implications of these subtypes. A biological pathway analysis of genes encoding differentially

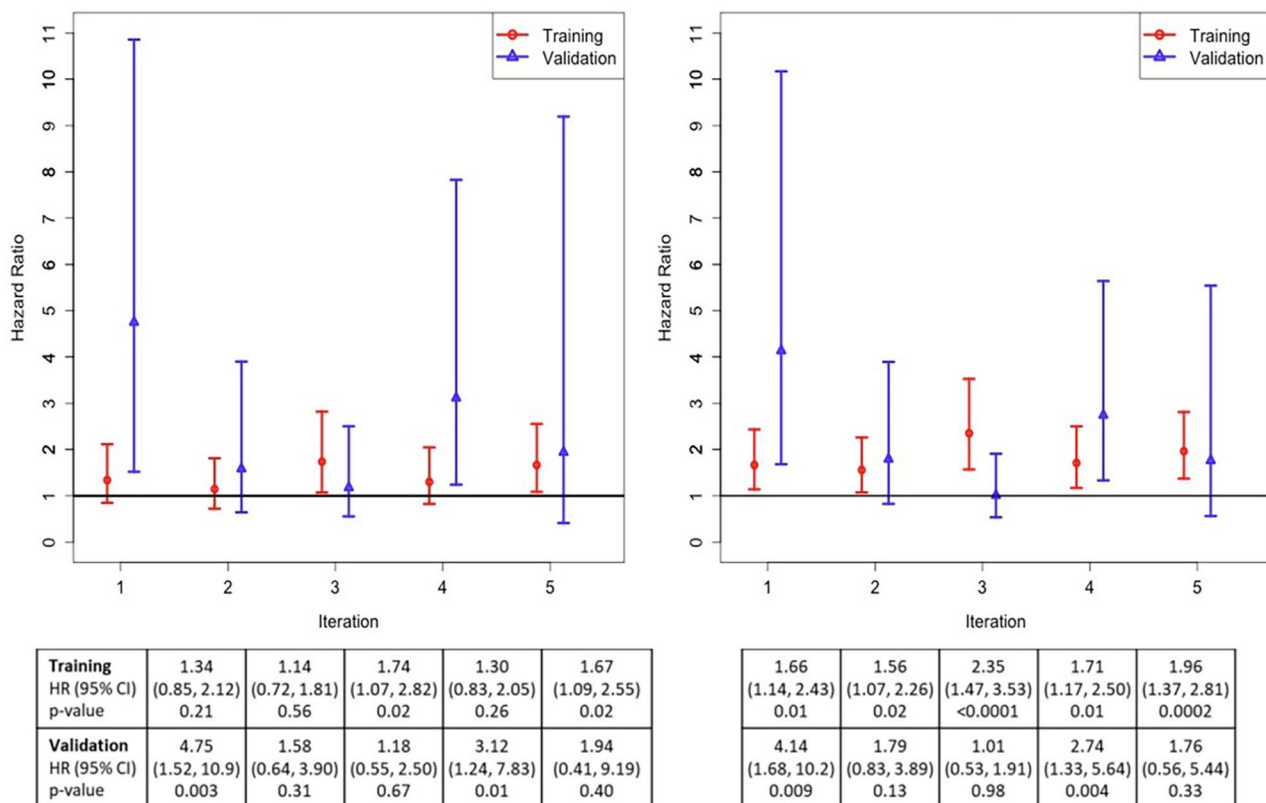


**Fig. 4** Random forest classification of subjects into molecular subtypes, based on the risk of experiencing the composite outcome of lung transplant or death (A), and the composite outcome of  $\geq 10\%$  absolute decline in FVC % predicted, lung transplant, or death (B) in each iteration of the cross-validation procedure. For all iterations, the HR was greater than 1, indicating a greater risk of these outcomes in subtype 1 compared to subtype 2. The associated tables show the HR, 95% CI, and p-values for each iteration in the training and validation datasets. HR: hazard ratio; CI: confidence interval

abundant proteins or regulated by the differentially expressed miRNAs suggested a coordinated alteration of gene expression among individuals at greater risk of disease progression, including in pathways previously associated with pulmonary fibrosis.

Accurate identification of patients with IPF who are likely to experience short-term disease progression has been proposed as part of an enrichment strategy for clinical trial design [41]. Previous studies have demonstrated associations between circulating levels of protein biomarkers and IPF prognosis; most of these studies measured a limited panel of proteins (selected based on disease mechanisms), or evaluated progression-free survival without considering disease progression [42–47]. Interestingly, two independent studies found that several neoepitopes of matrix metalloprotease-degraded extracellular matrix proteins or collagen synthesis were elevated in the blood of patients with progressive IPF relative to those with stable IPF [44, 45]. Another study used an aptamer-based platform for proteomic profiling of blood in patients with IPF, and identified 9 proteins associated with IPF progression [48]. Interestingly two (carbonic anhydrase XIII and NACA) were among the 232 proteins that we identified as differentially

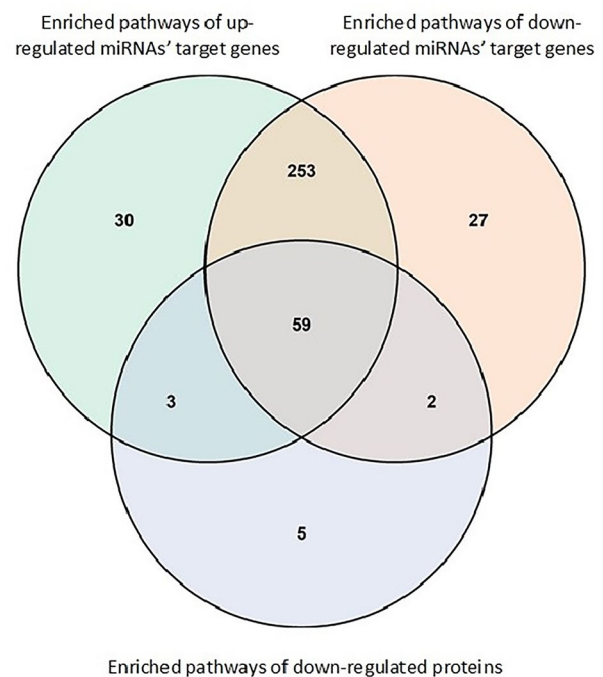
abundant in the IPF subtypes, but while we determined that lower abundance was associated with progression, this prior study found lower abundance to be protective [48]. Similarly, the 52-gene signature has been shown to predict transplant-free survival; however, its association with disease progression has not previously been tested [9, 10]. When applied in our cohort, the high-risk group based on the 52-gene signature experienced significantly shorter transplant-free survival (as expected), but did not experience shorter progression-free survival based on a composite of  $\geq 10\%$  absolute decline in FVC % predicted, lung transplant, or death. In contrast, our molecular subtype 1 experienced shortened progression-free survival after adjusting for disease severity and antifibrotic drug use at enrollment. This suggests better resolution to predict disease progression based on multi-omics rather than gene expression (toRNA) alone. While a recent analysis suggested that longitudinal change in peripheral blood gene expression predicted a  $\geq 10\%$  decrease in FVC over follow-up [49], risk ascertainment at a single time-point would be optimal, with the protein/miRNA classifier of IPF subtypes a candidate for further development and validation.

**Table 2** Molecules selected as classifiers of the molecular subtypes of IPF in at least 3 iterations

Molecule	Number of iterations in which molecule was selected	Variable importance across iterations where selected Mean (standard deviation)
GRB2 adapter protein	4	5.96 (1.47)
PKC-A	4	4.92 (2.16)
BCL2-like 1 protein	3	3.93 (3.26)
Sorting nexin 4	4	3.86 (1.67)
DUS3	3	3.29 (1.34)
IF4G2*	5	3.28 (2.29)
NDP kinase B*	5	3.25 (2.54)
GSK-3 alpha/beta	4	3.20 (1.42)
Cyclophilin F	3	2.97 (0.84)
DLRB1	3	2.96 (3.23)
FER	3	2.95 (2.06)
UFC1*	5	2.85 (0.91)
Caspase-3	4	2.70 (1.46)
14-3-3	3	2.66 (0.38)
PKB beta	3	2.41 (3.05)
Sphingosine kinase 1	4	2.26 (2.06)
PDE5A	4	2.19 (1.51)
HSP 60	3	2.14 (1.78)
Cofilin-1	3	2.02 (1.13)
SBDS	4	1.96 (0.62)
SMAD2	3	1.70 (0.73)
ERK-1	4	1.69 (0.95)
BARK1*	5	1.63 (0.78)
MAPK2	4	1.63 (0.99)
CSK	4	1.56 (1.01)
Calcineurin	4	1.50 (1.49)
PKB a/b/g	4	1.49 (0.72)
RAC1	3	1.48 (0.73)
IMB1	4	1.14 (0.69)
Aflatoxin B1 aldehyde reductase	3	1.02 (0.63)
Cytochrome P450 3A4	3	0.97 (0.80)
TEC	4	0.91 (0.46)
LYNB	3	0.83 (0.42)
XPNPEP1	3	0.73 (0.43)
hsa-miR-744-5p*	5	2.17 (1.33)
hsa-miR-199a-5p	3	1.94 (0.07)
hsa-miR-126-5p	3	1.61 (0.65)
hsa-miR-107	3	1.46 (0.38)
hsa-miR-3074-5p	3	1.21 (0.15)
hsa-miR-451a	3	1.15 (0.30)
hsa-miR-24-3p	3	1.10 (0.11)

\*Indicates a molecule selected in all 5 classifier iterations.

The larger the variable importance score, the more relevant the variable is to the prediction.

**Fig. 5** Overlap among the enriched pathways of down-regulated proteins, up-regulated target genes for miRNAs and down-regulated target genes for miRNAs.

Integrating high-throughput data from multiple platforms remains a challenge. In this study, we initially considered three methods based on two general approaches. iCluster+ and iClusterBayes include a variable selection step (i.e., lasso) followed by distillation of input matrices to a smaller set of latent variables, allowing joint clustering of samples and identification of cluster-relevant features [17, 31, 32]. Our two-step scSNF constructed a sample-similarity network (where each patient is a sample) for each omics data type and integrated these networks into a fused similarity network using a non-linear combination method [13], followed by unsupervised spectral clustering [32]. Importantly, the scSNF procedure omitted the variable selection step, limiting one source of bias.

The molecular subtypes that we identified based on integration of data from several constituents of the gene-to-protein expression pathway appear to reflect the pathobiology of IPF. Several of the proteins that were different in subtype 1 compared to 2 have been implicated in IPF pathogenesis. For example, activation of GSK-3 beta protein, which is reduced in molecular IPF subtype 1, is enhanced by TGF-beta, contributing to myofibroblast differentiation; GSK-3 beta signaling inhibition has been proposed as a treatment strategy for IPF [50]. PKB beta protein, reduced in subtype 1, has been implicated in the pathogenesis of IPF, where AKT2 knockout results in lower IL-13 and TGF-beta production by macrophages, alleviating fibrosis in animal models [51]. The



MAPK/ERK pathway, of which several protein constituents were reduced in subtype 1, is activated by TGF- $\beta$ , with ERK-1/2 linked with abnormal cellular senescence [52, 53]. MAPKAPK2 (MK2) is elevated in fibroblasts and epithelial cells from patients with IPF, and its inhibition has been proposed as a treatment strategy based on pre-clinical models [54]. Interestingly, we found decreased protein abundance in the peripheral blood of persons with IPF who were at increased risk for physiologic progression, while the literature suggests that reduced quantity or activity should be protective or therapeutic. It is possible that target tissue protein quantity or activity differs from blood, but these findings may have important implications for use of blood proteins as candidate biomarkers of disease stage and/or treatment response.

Several miRNAs that have been mechanistically linked with IPF were differentially expressed in molecular IPF subtype 1 compared to 2. We identified increased expression of mir-142-5p and reduced expression of mir-130a-3p in subtype 1. Altered expression of these miRNA in macrophages (in a similar direction as we observed) has been implicated in lung and liver fibrosis via reduced STAT6 signaling; mir-142-5p targets SOCS1 (a negative regulator of STAT6 phosphorylation), and mir-130a-3p targets the PPAR- $\gamma$  inhibitor [16]. We found reduced expression of miR-21-3p and increased expression of miR-21-5p in molecular subtype 1. Over-expression of miR-21 has been demonstrated in the lungs of patients with IPF and in animal models of lung fibrosis, suggesting it may function via reduction of Smad7, a downstream inhibitor of TGF- $\beta$  signaling [15]. We also observed differential expression of miR-34a-5p, miR-126-5p, and miR-199a-5p in molecular subtype 1 although the direction of differential expression did not always match that expected in IPF based on published literature [55–58].

To gain additional insight into biologic differences between the molecular subtypes, canonical pathways over-representation analysis (IPA) was conducted separately for up- and down-regulated molecules in subtype 1 compared to 2. The intersection of these datasets comprised a number of pathways known to be altered in IPF (e.g., VEGF, PDGF, ERK/MAP signaling [52–54, 59]). Among non-intersecting (across proteins and miRNA) pathways, multiple innate or adaptive immunity-related pathways were over-represented among target genes of miRNA that were down-regulated in progressive IPF. Pathways that were uniquely over-represented among target genes of up-regulated miRNA in progressive IPF included a number that were related to cellular or metabolic processes. Given that miRNA often act as post-transcriptional down-regulators of gene expression, this might suggest that IPF progression is associated with increased immune responses and decreased cellular metabolism. With miRNA not extensively studied in IPF,

additional research is needed to better understand these results.

Our study has several limitations. First, the aptamer-based proteomics platform we used contains a targeted list of biomarkers that is not comprehensive of all the proteins that may be found in the blood or potentially associated with pathobiology. Second, molecules measured in peripheral blood may not reflect the pathobiology of the target tissue [18, 19, 24]. Third, while this real-world registry followed participants to death or transplant, we cannot exclude the possibility that detection of disease progression based on only physiologic decline was impacted by informative missingness in lung function measurements (i.e., sicker patients were less able to complete testing). Finally, although we were able to internally validate (via resampling) our classifier of the molecular subtypes, the classifier of the molecular subtypes of IPF requires further development and validation in an independent cohort.

## Conclusions

In summary, we used a well-characterized, prospective, real-world cohort of patients with IPF to identify novel endotypes of IPF by integrating peripheral blood transcriptomic (toRNA, miRNA) and proteomic information. If externally validated, the classifier of patients with IPF to molecular subtype 1 or 2 could serve as a biomarker for prognostic enrichment in clinical trials. Constituents of the classifier, or pathways enriched among progression-associated molecules, could be explored further as therapeutic targets.

A podcast discussing these data and other analyses of circulating biomarkers in the IPF-PRO Registry is available at: <https://www.usccomms.com/respiratory/Todd/IPF-PROmultiomics>.

## Abbreviations

CPI	Composite physiologic index
DLco	Diffusion capacity of the lung for carbon monoxide
ECM	Extracellular matrix
FDR	False discovery rate
FEV1	Forced expiratory volume in the first second
FVC	Forced vital capacity
HR	Hazard ratio
IPF	Idiopathic pulmonary fibrosis
IPA	Ingenuity Pathway Analysis
MI	Myocardial infarction
miRNA	MicroRNA
NMI	Normalized Mutual Information
scSNF	Spectral clustering Similarity Network Fusion
toRNA	totalRNA

## Supplementary Information

The online version contains supplementary material available at <https://doi.org/10.1186/s12931-023-02435-0>.

**Additional file 1: Section S1.** Process used to quantify proteins, toRNA, and miRNA and perform bioinformatics analyses.

**Additional file 2: Table S1.** Number of tRNA, miRNA and proteomics features available for modeling after filtering and pre-processing.

**Additional file 3: Section S2.** Process used to develop classifier for molecular subtypes. **Figure S1.** Methods for development of classifier for molecular subtypes.

**Additional file 4: Section S3.** Differential expression analyses.

**Additional file 5: Figure S2.** Average Silhouette scores of consensus clustering for 2 to 10 clusters. **Section S4.** Multi-omics clustering by different methods. **Table S2.** Cluster membership consensus between scSNF and iClusterPlus or iClusterBayes. **Table S3.** Sensitivity analysis based on different variance filters for RNA-seq data. **Table S4.** Comparison of molecular subtypes based on scSNF with high-risk and low-risk groups based on the 52-gene signature. **Table S5.** Agreement (based on Normalized Mutual Information [NMI]) in distribution of subjects to molecular subtypes using a single molecule type compared to distribution using the scSNF fused multi-omics dataset. **Table S6.** Differentially abundant proteins by molecular subtype. **Table S7.** Differentially expressed miRNAs by molecular subtype.

**Additional file 6: Table S8.** Canonical pathways that were significantly enriched (FDR  $p$ -value < 0.05) for genes associated with down-regulated proteins.

**Additional file 7: Table S9.** Canonical pathways that were significantly enriched (FDR  $p$ -value < 0.05) for the experimentally-validated target genes of the 591 up-regulated and 1313 down-regulated miRNAs.

## Acknowledgements

We thank the principal investigators and enrolling centers in the IPF-PRO Registry: Albert Baker, Lynchburg Pulmonary Associates, Lynchburg, VA; Scott Beegle, Albany Medical Center, Albany, NY; John A Belperio, University of California Los Angeles, Los Angeles, CA; Rany Condos, NYU Medical Center, New York, NY; Francis Cordova, Temple University, Philadelphia, PA; Daniel A Culver, Cleveland Clinic, Cleveland, OH; Daniel Dilling, Loyola University Health System, Maywood, IL; John Fitzgerald (formerly Leann Silhan), UT Southwestern Medical Center, Dallas, TX; Kevin R Flaherty, University of Michigan, Ann Arbor, MI; Kevin Gibson, University of Pittsburgh, Pittsburgh, PA; Mridu Gulati, Yale School of Medicine, New Haven, CT; Kalpalatha Guntupalli, Baylor College of Medicine, Houston, TX; Nishant Gupta, University of Cincinnati Medical Center, Cincinnati, OH; Amy Hajari Case, Piedmont Healthcare, Atlanta, GA; David Hotchkin, The Oregon Clinic, Portland, OR; Tristan J Huie, National Jewish Health, Denver, CO; Robert J Kaner, Weill Cornell Medical College, New York, NY; Hyun J Kim, University of Minnesota, Minneapolis, MN; Lisa H Lancaster (formerly Mark Steele), Vanderbilt University Medical Center, Nashville, TN; Joseph A Lasky, Tulane University, New Orleans, LA; Doug Lee, Wilmington Health and PMG Research, Wilmington, NC; Timothy Liesching, Lahey Clinic, Burlington, MA; Randolph Lipchik, Froedtert & The Medical College of Wisconsin Community Physicians, Milwaukee, WI; Jason Lobo, UNC Chapel Hill, Chapel Hill, NC; Tracy R Luckhardt (formerly Joao A de Andrade), University of Alabama at Birmingham, Birmingham, AL; Yolanda Mageto (formerly Howard Huang), Baylor University Medical Center at Dallas, Dallas, TX; Marta Kokoszynska (formerly Yolanda Mageto, Prema Menon), Vermont Lung Center, Colchester, VT; Lake Morrison, Duke University Medical Center, Durham, NC; Andrew Namen, Wake Forest University, Winston Salem, NC; Justin M Oldham, University of California, Davis, Sacramento, CA; Tessy Paul, University of Virginia, Charlottesville, VA; David Zhang (formerly Anna Podolanczuk, David Lederer, Nina M Patel), Columbia University Medical Center/New York Presbyterian Hospital, New York, NY; Mary Porteous (formerly Maryl Kreider), University of Pennsylvania, Philadelphia, PA; Rishi Raj (formerly Paul Mohabir), Stanford University, Stanford, CA; Murali Ramaswamy, Pulmonix LLC, Greensboro, NC; Tonya Russell, Washington University, St. Louis, MO; Paul Sachs, Pulmonary Associates of Stamford, Stamford, CT; Zeenat Safdar, Houston Methodist Lung Center, Houston, TX; Shirin Shafazand (formerly Marilyn Glassberg), University of Miami, Miami, FL; Ather Siddiqi (formerly Wael Asi), Renovatio Clinical, The Woodlands, TX; Reginald Fowler (formerly Barry Sigal), Salem Chest and Southeastern Clinical Research Center, Winston Salem, NC; Mary E Strek (formerly Imre Noth), University of Chicago, Chicago, IL; Hiram Rivas-Perez (formerly Jesse Roman, Sally Suliman), University of Louisville, Louisville, KY; Jeremy Tabak, South Miami Hospital, South Miami, FL;

Rajat Walia, St. Joseph's Hospital, Phoenix, AZ; Timothy PM Whelan, Medical University of South Carolina, Charleston, SC. The authors thank Janine Roy, Staburo GmbH, Munich, Germany for conducting the primary analysis of the sequencing data and Naftali Kaminski and Jose D. Herazo-Maya from Yale University, New Haven, USA for confirming how the 52-gene signature should be applied. The authors meet criteria for authorship as recommended by the International Committee of Medical Journal Editors (ICMJE). The authors did not receive payment for development of this article. Editorial support was provided by Melanie Stephens and Wendy Morris of Fleishman-Hillard, London, UK, which was contracted and funded by Boehringer Ingelheim Pharmaceuticals, Inc. Boehringer Ingelheim was given the opportunity to review the article for medical and scientific accuracy as well as intellectual property considerations.

## Authors' contributions

The statistical analyses were discussed by P.R., Y.L. and H.Z. and performed by P.R. J.F.S. conducted the IPA analyses. P.R., J.L.T. and M.L.S. drafted the manuscript. All authors reviewed the manuscript and have approved the final version.

## Funding

The IPF-PRO/ILD-PRO Registry is supported by Boehringer Ingelheim Pharmaceuticals, Inc, and run in collaboration with the Duke Clinical Research Institute and enrolling centers.

## Data Availability

The datasets analyzed during the current study are not publicly available, but are available from the corresponding author on reasonable request.

## Declarations

### Ethics approval and consent to participate

The IPF-PRO Registry study obtained ethics approval at the data coordinating center (Duke Clinical Research Institute, Duke Institutional Review Board Protocol Number Pro00046131) and at every enrolling center (listed in the Acknowledgments). All participants gave informed consent. Additionally, ethics approval was granted by the Duke Institutional Review Board Protocol Number Pro00082241 to use the biosamples obtained as part of the IPF-PRO Registry for the analyses contained herein.

### Consent for publication

Not applicable.

### Competing interests

Peifeng Ruan, Hongyu Zhao and Mary Porteous have nothing to report. Jamie L Todd, Megan L Neely and Scott M Palmer are employees of the Duke Clinical Research Institute (DCRI) which receives funding support from Boehringer Ingelheim Pharmaceuticals, Inc. (BIPI) to coordinate the IPF-PRO/ILD-PRO Registry. Jamie L Todd also reports grants from AstraZeneca, BI, CareDx and has participated on Data Safety Monitoring Boards or Advisory Boards for Altavant Sciences, Natera, Theravance. Megan L Neely also reports honoraria for a lecture from North Carolina State University. Yi Liu, Richard Vinisko, Julia F Soellner, Ramona Schmid, Christian Hesslinger and Thomas B Leonard are employees of BI. Robert J Kaner reports grants paid to his institution from Bellerophon, BI, Genentech, the National Institutes of Health, Respivant, Toray, the US Department of Defense; royalties or licenses from UpToDate; consulting fees from AstraZeneca and Galapagos; speaker fees from BI, the France Foundation, Genentech, Vindico; has participated on Data Safety Monitoring Boards or Advisory Boards for BI, Genentech, Pliant, PureTech; holds unpaid leadership or fiduciary roles with the Pulmonary Wellness Foundation and the Stony Wold Foundation; holds stock or stock options with Air Cycle Systems and Doximity; and has received medical writing support from AstraZeneca, BI, Galapagos, Genentech. Tracy R Luckhardt reports grants from Bellerophon and FibroGen for her role as a clinical trial investigator. Imre Noth reports a contract for biospecimens from Veracyte; royalties from UpToDate; consulting fees from BI, Genentech, Sanofi; he holds a patent for a gene signature predictor of FVC and has a PCSK6 patent pending; he holds licenses for protein markers in IPF; he was a member of the Yale COVID Data Safety Monitoring Board. Rishi Raj has received an investigator-initiated research grant from BI and served on an advisory board for BI. Zeenat Safdar reports consulting fees and honoraria for lectures

from BI and Genentech. Mary E Strek has served as Principal Investigator for institutional and investigator-initiated grants from BI, and for institutional grants from Galapagos, Novartis, the Pulmonary Fibrosis Foundation; received honoraria for lectures and a textbook from CHEST; served on an adjudication committee for FibroGen; is on the American Thoracic Society Clinical Problems Committee and Research Innovation Summit Planning Committee; is Chair of the PFF Registry Scientific Review Committee. Scott M Palmer reports research funding to Duke/DCRI from AstraZeneca, Bristol Myers Squibb, CareDx; royalties or licenses from UpToDate; and speaker fees from Altavant Sciences, Bristol Myers Squibb, Mereo Biopharma, Theravance. Margaret L Salisbury reports grants paid to her institution from the National Institutes of Health; consulting fees from BI, Orinove Inc., Roche; payment for lectures from BI; and reimbursement to attend an investigators' meeting from BI.

#### Author details

<sup>1</sup>Department of Biostatistics, Yale School of Public Health, New Haven, CT, USA

<sup>2</sup>Duke Clinical Research Institute, Durham, NC, USA

<sup>3</sup>Duke University Medical Center, Durham, NC, USA

<sup>4</sup>Boehringer Ingelheim Pharmaceuticals, Inc, Ridgefield, CT, USA

<sup>5</sup>Boehringer Ingelheim Pharma GmbH & Co. KG, Biberach, Germany

<sup>6</sup>Weill Cornell Medicine, New York, NY, USA

<sup>7</sup>Department of Medicine, University of Alabama at Birmingham, Birmingham, AL, USA

<sup>8</sup>Division of Pulmonary and Critical Care Medicine, University of Virginia, Charlottesville, VA, USA

<sup>9</sup>Hospital of the University of Pennsylvania, Philadelphia, PA, USA

<sup>10</sup>Stanford University School of Medicine, Stanford, CA, USA

<sup>11</sup>Houston Methodist Lung Center, Houston, TX, USA

<sup>12</sup>Section of Pulmonary and Critical Care Medicine, University of Chicago, Chicago, IL, USA

<sup>13</sup>Department of Medicine, Vanderbilt University Medical Center, 1211 Medical Center Drive, 37232 Nashville, TN, USA

Received: 27 October 2022 / Accepted: 26 April 2023

Published online: 31 May 2023

#### References

- Raghu G, Remy-Jardin M, Richeldi L, Thomson CC, Inoue Y, Johkoh T, et al. Idiopathic pulmonary fibrosis (an update) and progressive pulmonary fibrosis in adults: an official ATS/ERS/JRS/ALAT clinical practice guideline. *Am J Respir Crit Care Med*. 2022;205(9):e18–47.
- Noth I, Zhang Y, Ma SF, Flores C, Barber M, Huang Y, et al. Genetic variants associated with idiopathic pulmonary fibrosis susceptibility and mortality: a genome-wide association study. *Lancet Respir Med*. 2013;1(4):309–317.
- Fingerlin TE, Murphy E, Zhang W, Peljto AL, Brown KK, Steele MP, et al. Genome-wide association study identifies multiple susceptibility loci for pulmonary fibrosis. *Nat Genet*. 2013;45(6):613–620.
- Roy MG, Livraghi-Buttrico A, Fletcher AA, McElwee MM, Evans SE, Boerner RM, et al. Muc5b is required for airway defence. *Nature*. 2014;505(7483):412–416.
- O'Dwyer DN, Norman KC, Xia M, Huang Y, Gurczynski SJ, Ashley SL, et al. The peripheral blood proteome signature of idiopathic pulmonary fibrosis is distinct from normal and is associated with novel immunological processes. *Sci Rep*. 2017;7:46560.
- Todd JL, Neely ML, Overton R, Durham K, Gulati M, Huang H, et al. Peripheral blood proteomic profiling of idiopathic pulmonary fibrosis biomarkers in the multicentre IPF-PRO Registry. *Respir Res*. 2019;20(1):227.
- Yang IV, Coldren CD, Leach SM, Seibold MA, Murphy E, Lin J, et al. Expression of cilium-associated genes defines novel molecular subtypes of idiopathic pulmonary fibrosis. *Thorax*. 2013;68(12):1114–1121.
- Yang IV, Luna LG, Cotter J, Talbert J, Leach SM, Kidd R, et al. The peripheral blood transcriptome identifies the presence and extent of disease in idiopathic pulmonary fibrosis. *PLoS One*. 2012;7(6):e37708–e37708.
- Herazo-Maya JD, Noth I, Duncan SR, Kim S, Ma SF, Tseng GC, et al. Peripheral blood mononuclear cell gene expression profiles predict poor outcome in idiopathic pulmonary fibrosis. *Sci Transl Med*. 2013;5(205):205ra136.
- Herazo-Maya JD, Sun J, Molyneaux PL, Li Q, Villalba JA, Tzouvelekis A, et al. Validation of a 52-gene risk profile for outcome prediction in patients with idiopathic pulmonary fibrosis: an international, multicentre, cohort study. *Lancet Respir Med*. 2017;5(11):857–868.
- Bowman WS, Newton CA, Linderholm AL, Neely ML, Pugashetti JV, Kaul B, et al. Proteomic biomarkers of progressive fibrosing interstitial lung disease: a multicentre cohort analysis. *Lancet Respir Med*. 2022;S2213-2600(21)00503-8.
- Kraven LM, Taylor AR, Molyneaux PL, Maher TM, McDonough JE, Mura M, et al. Cluster analysis of transcriptomic datasets to identify endotypes of idiopathic pulmonary fibrosis. *Thorax*. 2022;thoraxjnl-2021-218563.
- Baek D, Villen J, Shin C, Camargo FD, Gygi SP, Bartel DP. The impact of microRNAs on protein output. *Nature*. 2008;455(7209):64–71.
- Herrera J, Beisang DJ, Peterson M, Forster C, Gilbertsen A, Benyumov A, et al. Dicer1 deficiency in the idiopathic pulmonary fibrosis fibroblastic focus promotes fibrosis by suppressing microRNA biogenesis. *Am J Respir Crit Care Med*. 2018;198(4):486–496.
- Liu G, Friggeri A, Yang Y, Milosevic J, Ding Q, Thannickal VJ, et al. miR-21 mediates fibrogenic activation of pulmonary fibroblasts and lung fibrosis. *J Exp Med*. 2010;207(8):1589–1597.
- Su S, Zhao Q, He C, Huang D, Liu J, Chen F, et al. Mir-142-5p and miR-130a-3p are regulated by IL-4 and IL-13 and control profibrogenic macrophage program. *Nat Commun*. 2015;6:8523.
- Shen R, Olshen AB, Ladanyi M. Integrative clustering of multiple genomic data types using a joint latent variable model with application to breast and lung cancer subtype analysis. *Bioinformatics*. 2009;25(22):2906–2912.
- Curtis C, Shah SP, Chin SF, Turashvili G, Rueda OM, Dunning MJ, et al. The genomic and transcriptomic architecture of 2,000 breast tumours reveals novel subgroups. *Nature*. 2012;486(7403):346–352.
- Cancer Genome Atlas Research Network. Comprehensive and integrative genomic characterization of hepatocellular carcinoma. *Cell*. 2017;169(7):1327–1341.
- Cancer Genome Atlas Research Network. Comprehensive molecular characterization of papillary renal-cell carcinoma. *N Engl J Med*. 2016;374(2):135–145.
- Cancer Genome Atlas Network. Comprehensive molecular characterization of human colon and rectal cancer. *Nature*. 2012;487(7407):330–330.
- Konigsberg IR, Borie R, Walts AD, Cardwell J, Rojas M, Metzger F, et al. Molecular signatures of idiopathic pulmonary fibrosis. *Am J Respir Cell Mol Biol*. 2021;65(4):430–441.
- Gangwar I, Kumar Sharma N, Panzade G, Awasthi S, Agrawal A, Shankar R. Detecting the molecular system signatures of idiopathic pulmonary fibrosis through integrated genomic analysis. *Sci Rep*. 2017;7(1):1554.
- Kim S, Herazo-Maya JD, Kang DD, Juan-Guardela BM, Tedrow J, Martinez FJ, et al. Integrative phenotyping framework (iPF): integrative clustering of multiple omics data identifies novel lung disease subphenotypes. *BMC Genomics*. 2015;16:924.
- Casanova NG, Zhou T, Gonzalez-Garay ML, Lussier YA, Sweiss N, Ma SF, et al. MicroRNA and protein-coding gene expression analysis in idiopathic pulmonary fibrosis yields novel biomarker signatures associated to survival. *Transl Res*. 2021;228:1–12.
- O'Brien EC, Durham MT, Gamerman, Garfinkel S, Anstrom KJ, Palmer SM, et al. Rationale for and design of the idiopathic pulmonary fibrosis-prospective outcomes (IPF-PRO) registry. *BMJ Open Respir Res*. 2016;3(1):e000108.
- Wang B, Mezlini AM, Demir F, Fiume M, Tu Z, Brudno M, et al. Similarity network fusion for aggregating data types on a genomic scale. *Nature Methods*. 2014;11:333–337.
- Ng AY, Jordan MI, Weiss Y. On spectral clustering: analysis and an algorithm. *Adv Neural Inf Proc Syst*. 2002;2:849–856.
- Monti S, Tamayo P, Mesirov J, Golub T. Consensus clustering: a resampling-based method for class discovery and visualization of gene expression microarray data. *Machine learning*. 2003;52:91–118.
- Rousseeuw P. J. Silhouettes: A graphical aid to the interpretation and validation of cluster analysis. *Comput Appl Math*. 1987;20:53–65.
- Mo Q, Wang S, Seshan VE, Olshen AB, Schultz N, Sander C, et al. Pattern discovery and cancer gene identification in integrated cancer genomic data. *PNAS*. 2013;110:4245–4250.
- Mo Q, Shen R, Guo C, Vannucci M, Chan KS, Hilsenbeck SG. A fully bayesian latent variable model for integrative clustering analysis of multi-type omics data. *Biostatistics*. 2018;19(1):71–86.
- Raghu G, Collard HR, Anstrom KJ, Flaherty KR, Fleming TR, King Jr TE, et al. Idiopathic pulmonary fibrosis: clinically meaningful primary endpoints in phase 3 clinical trials. *Am J Respir Crit Care Med*. 2012;185(10):1044–1048.
- Wells AU, Desai SR, Rubens MB, Goh NS, Cramer D, Nicholson AG, et al. Idiopathic pulmonary fibrosis: a composite physiologic index derived from

- disease extent observed by computed tomography. *Am J Respir Crit Care Med.* 2003;167(7):962–969.
35. Romano S, Bailey J, Nguyen V, Verspoor K. Standardized mutual information for clustering comparisons: one step further in adjustment for chance. *PMLR* 2014;32(2):1143–1151.
  36. Ho TK. Random decision forests. In Proceedings of the 3rd International Conference on Document Analysis and Recognition, Montreal, Canada, August 14–18, 1995: 278–282.
  37. Krämer A, Green J, Pollard Jr J, Tugendreich S. Causal analysis approaches in ingenuity pathway analysis. *Bioinformatics.* 2014;30(4):523–530.
  38. Benjamini Y, Hochberg Y. Controlling the false discovery rate: a practical and powerful approach to multiple hypothesis testing. *J R Statist Soc.* 1995;57(1):289–300.
  39. Ley B, Ryerson CJ, Vittinghoff E, Ryu JH, Tomassetti S, Lee JS, et al. A multidimensional index and staging system for idiopathic pulmonary fibrosis. *Ann Intern Med.* 2012;156:684–691.
  40. Raghu G, Collard HR, Egan JJ, Martinez FJ, Behr J, Brown KK, et al. An official ATS/ERS/JRS/ALAT statement: idiopathic pulmonary fibrosis: evidence-based guidelines for diagnosis and management. *Am J Respir Crit Care Med.* 2011;183(6):788–824.
  41. Salisbury ML, Lynch DA, van Beek EJ, Kazerooni EA, Guo J, Xia M, et al. Idiopathic pulmonary fibrosis: the association between the adaptive multiple features method and fibrosis outcomes. *Am J Respir Crit Care Med.* 2017;195(7):921–929.
  42. Maher TM, Oballa E, Simpson JK, Porte J, Habgood A, Fahy WA, et al. An epithelial biomarker signature for idiopathic pulmonary fibrosis: an analysis from the multicentre PROFILE cohort study. *Lancet Respir Med.* 2017;5(12):946–955.
  43. Richards TJ, Kaminski N, Baribaud F, Flavin S, Brodmerkel C, Horowitz D, et al. Peripheral blood proteins predict mortality in idiopathic pulmonary fibrosis. *Am J Respir Crit Care Med.* 2012;185(1):67–76.
  44. Jenkins RG, Simpson JK, Saini G, Bentley JH, Russell AM, Braybrooke R, et al. Longitudinal change in collagen degradation biomarkers in idiopathic pulmonary fibrosis: an analysis from the prospective, multicentre PROFILE study. *Lancet Respir Med.* 2015;3(6):462–472.
  45. Organ LA, Duggan AR, Oballa E, Taggart SC, Simpson JK, Kang'ombe AR, et al. Biomarkers of collagen synthesis predict progression in the PROFILE idiopathic pulmonary fibrosis cohort. *Respir Res.* 2019;20(1):148.
  46. Adegunsoye A, Alqalyoobi S, Linderholm A, Bowman WS, Lee CT, Pugashetti JV, et al. Circulating plasma biomarkers of survival in antifibrotic-treated patients with idiopathic pulmonary fibrosis. *Chest.* 2020;158(4):1526–1534.
  47. Todd JL, Neely ML, Overton R, Mulder H, Roman J, Lasky JA, et al. Association of circulating proteins with death or lung transplant in patients with idiopathic pulmonary fibrosis in the IPF-PRO Registry cohort. *Lung.* 2022;200(1):19.
  48. Ashley SL, Xia M, Murray S, O'Dwyer DN, Grant E, White ES, et al. Six-SOMer index relating to immune, protease and angiogenic functions predicts progression in IPF. *PLoS One* 2016;11(8):e0159878.
  49. Huang Y, Oldham JM, Ma SF, Unterman A, Liao SY, Barros AJ, et al. Blood transcriptomics predicts progression of pulmonary fibrosis and associated natural killer cells. *Am J Respir Crit Care Med.* 2021;204(2):197–208.
  50. Jeffers A, Qin W, Owens S, Koenig KB, Komatsu S, Giles FJ, et al. Glycogen synthase kinase-3beta inhibition with 9-ING-41 attenuates the progression of pulmonary fibrosis. *Sci Rep.* 2019;9(1):18925.
  51. Nie Y, Sun L, Wu Y, Yang Y, Wang J, He H, et al. AKT2 regulates pulmonary inflammation and fibrosis via modulating macrophage activation. *J Immunol.* 2017;198(11):4470–4480.
  52. Chen H, Chen H, Liang J, Gu X, Zhou J, Xie C, et al. TGF-beta1/IL-11/MEK/ERK signaling mediates senescence-associated pulmonary fibrosis in a stress-induced premature senescence model of Bmi-1 deficiency. *Exp Mol Med.* 2020;52(1):130–151.
  53. Ard S, Reed EB, Smolyaninova LV, Orlov SN, Mutlu GM, Guzy RD, et al. Sustained SMAD2 phosphorylation is required for myofibroblast transformation in response to TGF-beta. *Am J Respir Cell Mol Biol.* 2019;60:367–369.
  54. Vittal R, Fisher A, Gu H, Mickler EA, Panitch A, Lander C, et al. Peptide-mediated inhibition of mitogen-activated protein kinase-activated protein kinase-2 ameliorates bleomycin-induced pulmonary fibrosis. *Am J Respir Cell Mol Biol.* 2013;49(1):47–57.
  55. Cui H, Ge J, Xie N, Banerjee S, Zhou Y, Antony VB, et al. miR-34a inhibits lung fibrosis by inducing lung fibroblast senescence. *Am J Respir Cell Mol Biol.* 2017;56(2):168–178.
  56. Pandit KV, Corcoran D, Yousef H, Yarlagaadda M, Tzouveleakis A, Gibson KF, et al. Inhibition and role of let-7d in idiopathic pulmonary fibrosis. *Am J Respir Crit Care Med.* 2010;182(2):220–229.
  57. Yang G, Yang L, Wang W, Wang J, Wang J, Xu Z. Discovery and validation of extracellular/circulating microRNAs during idiopathic pulmonary fibrosis disease progression. *Gene.* 2015;562(1):138–144.
  58. Lino Cardenas CL, Henaoui IS, Courcot E, Roderburg C, Cauffiez C, Aubert S, et al. miR-199a-5p is upregulated during fibrogenic response to tissue injury and mediates TGFbeta-induced lung fibroblast activation by targeting caveolin-1. *PLoS Genet.* 2013;9(2):e1003291.
  59. Amano H, Matsui Y, Hatanaka K, Hosono K, Ito Y. VEGFR1-tyrosine kinase signaling in pulmonary fibrosis. *Inflamm Regen.* 2021;41(1):16.

## Publisher's Note

Springer Nature remains neutral with regard to jurisdictional claims in published maps and institutional affiliations.